Toward Thermally, Oxidatively, and Spectrally Stable Polyfluorene-Based Materials: Aromatic Ether-Functionalized Polyfluorene

Shaune L. McFarlane,[†] Davin G. Piercey,[†] Leah S. Coumont,[†] Ryan T. Tucker,[‡] Michael D. Fleischauer,[§] Michael J. Brett,[‡,§] and Jonathan G. C. Veinot*,[†]

Department of Chemistry, University of Alberta, Edmonton, Alberta T6G 2G2, Canada; Department of Electrical and Computer Engineering, University of Alberta, Edmonton, Alberta T6G 2V4, Canada; and NRC-National Institute for Nanotechnology, 11421 Saskatchewan Dr., Edmonton, Alberta T6G 2M9, Canada

Received October 6, 2008; Revised Manuscript Received December 1, 2008

ABSTRACT: Two unique fluorene monomers (PTE and MTE) and polyfluorene-based homopolymers (PPTE and PMTE) containing covalently linked aromatic ether (AE) moieties were synthesized via microwave Ni(0)-mediated Yamamoto coupling reactions. The monomers and polymers demonstrated thermal stabilities, as determined by TGA, much higher than status quo poly(9,9′-dioctylfluorene) (PFO) (i.e., greater than 100 °C), and most importantly, the spectral emission remained stable after annealing in ambient and inert atmospheres. PPTE and PMTE were annealed in an N_2 atmosphere at 200 °C for 72 h and at 150 °C in ambient atmosphere for 1 h showing no evidence of green emission, in stark contrast to PFO. The results show that PFs with AE moieties present in the 9-position exhibit stable blue emission.

Introduction

Blue-emitting polyfluorene (PF) polymers are being pursued as active materials in polymer light-emitting diodes,[1] lasers,[2–6] and sensors.[7–12] To meet the requirements of practical device application, high-molecular-weight blue-emitting poly(*p*-phenylene) (PPP) materials including, ladder-type PPPs,[13] polyfluorenes (PF),[14] polyindenofluorenes (PIFs),[15] and polytetrahydrophenanthrene (PTHP)[16] have being widely investigated. Alkyl-substituted PFs, such as poly(9,9′-dioctylfluorene) (PFO), are among the most promising candidates for optoelectronic applications.[17] Still, the inherent spectral instability of alkyl-substituted PFs (i.e., green emission upon exposure to thermal stressing) remains a significant challenge limiting full realization of their potential.

It is now well-established that the primary source of the undesirable green emission is fluorenone defects formed during and/or after polymer synthesis.[18] Attempts to prevent defect formation have included derivatization at the 9-position with trifluoromethyl,[19] silole,[20] siloxane,[21] silsesquioxane,[22] polyphenylene,[23] and dendritic benzyl ether[24] moieties. These studies clearly show that controlling the molecular structure of PF at the 9-position affords a viable solution toward improving material performance. In addition to functionalizing the 9-position, the preparation of carbazole backbone-functionalized PF polymers has also been shown to decrease this green emission.[25]

PAEs are well-known engineering thermoplastics possessing excellent thermal, chemical, radiation, and oxidative stability.[26,27] In this regard, it is reasonable that their incorporation into PF-based materials will lead to increased spectral stability. Jiang et al. prepared a series of poly(aryl ether) (PAE) polymers bearing pendent alkyl-substituted oligofluorenes.[28,29] As a result of incorporating aromatic ethers (AEs) into the polymer backbone, they prepared hybrid materials exhibiting increased spectral stability when annealed in vacuum. Annealing studies in ambient conditions were not reported for these systems; hence, their oxidative stability remains unknown.

* Corresponding author. E-mail: jveinot@ualberta.ca.
[†] Department of Chemistry, University of Alberta.
[‡] Department of Electrical and Computer Engineering, University of Alberta.
[§] NRC-National Institute for Nanotechnology.

To date, grafting AE functionalities to the 9-position of fluorene has not been investigated as a mode for increasing thermal, oxidative, and spectral stabilization of PFs. It is reasonable that this absence from the literature is a direct consequence of challenges associated with preparing wholly AE bonds. A search of the literature reveals a limited number of general methodologies for preparing this moiety.

Two classical methods for preparing AEs are the copper-mediated Ullmann ether synthesis[30,31] and electron-withdrawing group (EWG) facilitated nucleophilic aromatic substitution (S_NAr) protocols.[26,32] These approaches are generally ineffective in preparing high-purity materials for organic electronics (e.g., PLEDs) because elevated temperatures, copper salts, and EWGs are required for the reaction to go to completion and difficult to remove from the product. In addition, it is difficult to prepare materials in a controlled stepwise fashion, thereby limiting control over subtle changes in molecular structure. Fine structural control is well-known to dramatically impact material properties; therefore, a synthetic method that can accomplish this would be ideal.

S_NAr protocols utilizing transition-metal-mediated activation of aromatic rings have recently gained popularity as methods for preparing AE bonds. In particular, iron-based methodologies utilizing cyclopentadienyliron ($CpFe^+$) as activating groups, first discovered by Nesmeyanov et al.[33] have been employed in the preparation of AE bonds in a controlled stepwise fashion.[34–37] Syntheses are typically performed at room temperature, and the $CpFe^+$ moiety, acting as a temporary auxiliary agent, is readily removed, leaving behind wholly AE-containing material. This approach allows for mild, stepwise access to AE bonds. In this report, we show the above methodology may be utilized in preparing AE-containing fluorene monomers that, upon polymerization utilizing microwave-initiated Yamamoto coupling,[38] generates blue-emitting AE-functionalized PFs. Thermogravimetric analysis (TGA) and thermal oxidative degradation studies in ambient confirm that the incorporation of AE units at the 9-position substantially improves the thermal, oxidative, and color stability of these new materials when compared to status quo alkyl-functionalized PFs (i.e., PFO). The inclusion of AE

10.1021/ma8022348 CCC: $40.75
Published on Web 01/06/2009

Scheme 1. Synthesis of 2,7-Dibromo-9,9′-di(4-hydroxyphenyl)-9*H*-fluorene Target Precursor (3)[a]

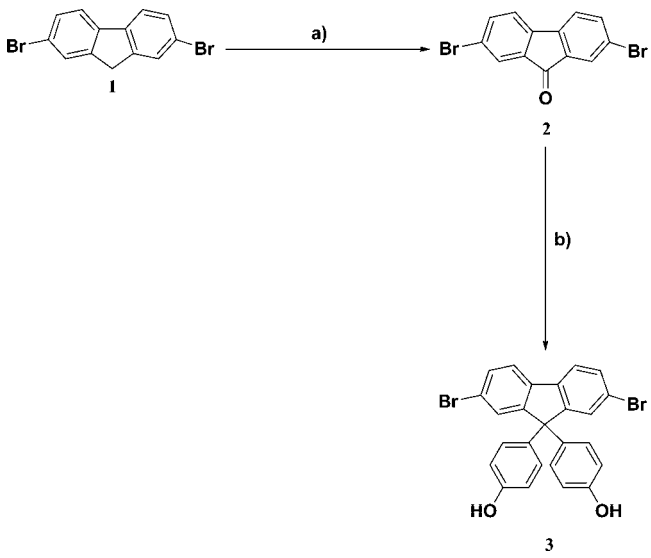

[a] (a) CrO_3, ethyl acetate, stir for 24 h; (b) phenol, methanesulfonic acid, 3-mercaptopropionic acid, 70 °C for 20 h.

structural units provides a straightforward approach toward eliminating adverse effects of thermal degradation of PF materials.

Experimental Section

General Information. All reagents and solvents were purchased from commercial sources and used without further purification unless specified. Potassium carbonate was purchased from Mallinckrodt; concentrated HCl was purchased from EMD; dimethylformamide (DMF), acetic anhydride, toluene, >99% phenol, 98% ferrocene, 99% aluminum chloride, 99.99% ammonium hexafluorophosphate, 99.9% chromium(VI) oxide, 99+% 1,4-dichlorobenzene, 98% 1,3-dichlorobenzene, anhydrous 99% 1,5-cyclooctadiene (cod), >99% 2,2′-bipyridyl (bpy) dried on a Schlenk line for 16 h, and 97% 5-bromo-*m*-xylene were purchased from Aldrich; diethyl ether, methanol, acetone, ethyl acetate, hexane, and 2,7-dibromofluorene (**1**) were purchased from Alfa Aesar; 98% $Ni(cod)_2$ and 99.7% aluminum powder were purchased from Strem; 2,7-dibromofluorene-9-one[39] (**2**), 2,7-dibromo-9,9′-bis(4-hydroxyphenyl)-9*H*-fluorene[40] (**3**), η^6-1,4-dichlorobenzene−η^5-cyclopentadienyliron hexafluorophosphate[42] (**4a**), and η^6-1,3-dichlorobenzene−η^5-cyclopentadienyliron hexafluorophosphate[42] (**4b**) were prepared according to literature procedures. **5b** was not isolated. Microwave syntheses were carried out with a Biotage Initiator system. ^{1}H NMR and ^{13}C NMR spectra were recorded with a Varian Inova 400 (400 and 100 MHz, respectively) and Varian 500 (500 and 125 MHz, respectively) spectrometers. Elemental analysis was performed with a Carlo Erba CHNS-O EA1108 elemental analyzer. Photoluminescence (PL) spectra were obtained with a Varian Cary Eclipse fluorescence spectrophotometer. UV−vis spectra were obtained with an Agilent 8453 UV−vis spectrophotometer. Low-resolution mass spectrometry was performed with an Applied Biosystems Voyager Elite matrix-assisted laser desorption time-of-flight (MALDI-TOF) system, and high-resolution mass spectrometry was performed with a Bruker 9.4T Fourier transform ion cyclotron resonance (FTICR) system and an Applied Biosystems Mariner orthogonal acceleration time-of-flight (ao-TOF) system. Thermogravimetric analysis (TGA) was performed on a Perkin-Elmer Pyris 1 system at a heating rate of 10 °C/min. Differential scanning calorimetry (DSC) was performed with a TA Instruments Q1000 system at various heating and cooling rates. GPC analysis was performed on an Agilent 1100 series system equipped with a Waters Styragel HR 4E column.

PLED Fabrication/Electroluminescence Testing. Indium−tin oxide (ITO)-coated glass substrates (8−12 Ω/sq, Delta Tech.) were sonicated in IPA, dried at 120 °C, and exposed to an O_2 plasma for 1 min. Hole injection PEDOT/PSS (Aldrich) was applied from a 2.8% w/v aqueous solution and heated at 60 °C for 10 min in a class 10 cleanroom. Active layers were prepared from 0.5% w/v toluene solutions and heated at 70 °C for 15 min in an N_2-filled glovebox. Electrical contacts were fabricated by sequentially depositing ca. 5 nm of Ca and ca. 150 nm of Al. PLED electroluminescence spectra were obtained in air using a Varian Cary Eclipse fluorescence spectrophotometer. IV curves were collected using a computer-controlled Keithley 2400 source.

Monomer and Polymer Synthesis. *Synthesis of PIBC (**5a**).* 2,7-Dibromo-9,9′-bis(4-hydroxyphenyl)-9*H*-fluorene (4.98 g, 9.72 mmol), η^6-1,4-dichlorobenzene−η^5-cyclopentadienyliron hexafluorophosphate (8.03 g, 19.44 mmol), and potassium carbonate (2.69 g, 19.44 mmol) along with 100 mL of DMF were combined in a 250 mL round-bottom flask. The dark brown solution was covered with aluminum foil and stirred under an argon atmosphere at 50 °C for 24 h. The resulting purple solution was poured into 1200 mL of a 10% HCl(aq) solution, yielding a yellow precipitate. Ammonium hexafluorophosphate (3.17 g, 19.44 mmol) was dissolved in distilled water and added to the yellow precipitate to ensure complete precipitation. The yellow precipitate was collected over a Buchner funnel and washed with copious amounts of distilled water. When completely dry, the powder was washed a further three times with a total of 200 mL of diethyl ether, giving a pale yellow powder (10.12 g, 83%). ^{1}H NMR (400 MHz, d_6-DMSO): δ 8.00 (d, J = 8.0 Hz, 2 H); 7.68 (m, J = 8.0 Hz, 4 H); 7.28 (m, J = 8.8 Hz, 8 H); 6.79 (d, J = 6.4 Hz, 4 H); 6.43 (d, J = 6.4 Hz, 4 H); 5.25 (s, 10 H). ^{13}C NMR (100 MHz, d_6-DMSO): δ 152.21, 152.07, 141.78, 137.72, 131.49, 131.44, 129.84, 128.65, 123.10, 121.51, 120.54, 103.59, 86.74, 79.31, 76.51, 64.23. HRMS Calculated for $C_{47}H_{32}O_2Br_2Fe_2$ [M^{2+} = M-2PF_6]: 967.883 39. Found: 967.882 02. Elemental Analysis for $C_{47}H_{32}O_2Cl_2Br_2Fe_2P_2F_{12}$: C, 44.76; H, 2.56. Found: C, 45.67; H, 2.95.

*Synthesis of PFBC (**6a**).* 2,7-Dibromo-9,9′-bis(4-hydroxyphenyl)fluorene (2.00 g, 3.94 mmol), η^6-1,4-dichlorobenzene−η^5-cyclopentadienyliron hexafluorophosphate (3.30 g, 7.99 mmol), and potassium carbonate (1.6 g, 11.6 mmol) along with 80 mL of DMF were combined in a 500 mL round-bottom flask. The green/brown solution was covered with aluminum foil and stirred under an argon atmosphere at room temperature for 24 h. Potassium carbonate (1.6 g, 11.6 mmol) and phenol (0.80 g, 8.5 mmol) along with an additional 40 mL of DMF was added to the solution and allowed to stir for an additional 72 h. The resultant brown solution was poured into 800 mL of a 10% HCl(aq) solution, forming a yellow precipitate. The yellow solid was collected over a Buchner funnel and washed with copious amounts of distilled water. When completely dry, the solid was washed with ~600 mL of diethyl ether, giving a yellow powder (5.35 g, 99%). ^{1}H NMR (500 MHz, d_6-DMSO): δ 7.99 (d, J = 8.1 Hz, 2 H); 7.68−7.48 (m, 8 H); 7.40−7.14 (m, 14 H); 6.28 (m, 8 H); 5.20 (s, 10 H). ^{13}C NMR (125 MHz, d_6-DMSO): δ 153.30, 152.85, 151.11, 141.39, 137.69, 131.41, 130.67, 130.13, 129.74, 129.45, 128.61, 126.19, 123.11, 121.47, 120.36, 120.23, 77.86, 75.47, 74.96, 64.17. Elemental Analysis for $C_{59}H_{42}O_4Br_2Fe_2P_2F_{12}$: C, 51.49; H, 3.08. Found: C, 50.20; H, 3.18.

*Synthesis of MFBC (**6b**).* 2,7-Dibromo-9,9′-bis(4-hydroxyphenyl)-9*H*-fluorene (1.03 g, 2.03 mmol), η^6-1,3-dichlorobenzene−η^5-cyclopentadienyliron hexafluorophosphate (1.65 g, 4.00 mmol), and potassium carbonate (0.80 g, 5.79 mmol) along with 40 mL of DMF were combined in a 100 mL round-bottom flask. The dark brown solution was covered with aluminum foil and stirred under an argon atmosphere at room temperature for 24 h. Potassium carbonate (0.8 g, 5.79 mmol) and phenol (0.4 g, 4.24 mmol) along with an additional 20 mL of DMF were added to the brown/black solution and allowed to stir for an additional 72 h. The resulting dark orange solution was poured into 400 mL of a 10% HCl(aq) solution, producing an orange/beige precipitate. After stirring for a few minutes, the precipitate was collected over a Buchner funnel and

Scheme 2. Synthesis of PTE and MTE Monomers via $CpFe^+$ Activation (7a or 7b)[a]

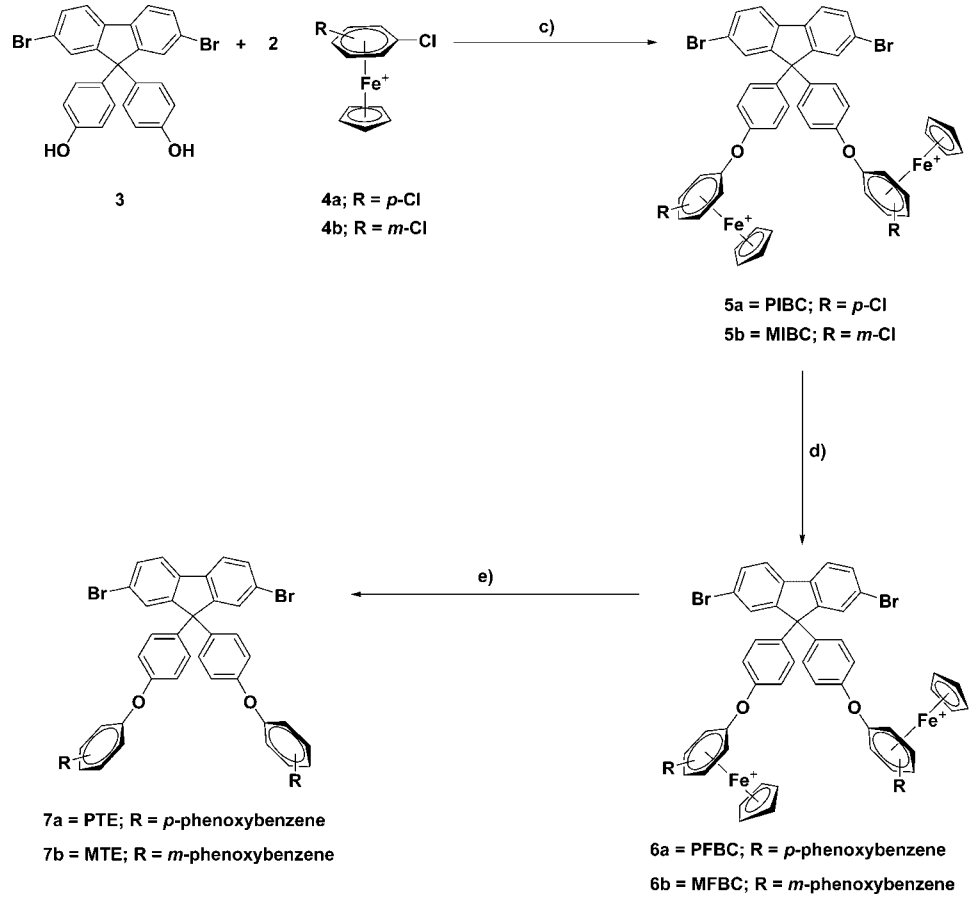

[a] (c) K_2CO_3, dissolve **3** and **4a** or **4b** in DMF, stir at room temperature for 24 h, isolation of **5a** and **5b** is not necessary prior to proceeding to the next synthetic step; (d) K_2CO_3, phenol, more DMF, stir at room temperature for 72 h; (e) dissolve **6a** and **6b** in DMF and CH_3CN, dimethylglyoxime and heat for 12 min at 200 °C in a microwave reactor.

Table 1. Melting Temperature (T_m), Glass Transition Temperature (T_g), (Purity, and Decomposition Temperature (T_d) under both N_2 and Air of MTE and PTE Monomers

monomer	T_m (°C)[a]	purity[b]	T_d (°C) N_2[c]	T_d (°C) air[d]	T_g[e] (°C)
MTE	175	95.3	418	415	53
PTE	166	96.5	443	445	78

[a] T_m was determined with DSC at a heating rate of 0.5 °C/min with 1−3 mg of sample. [b] Calorimetric purity determinations were made using 1−3 mg samples heated at 0.5 °C/min with a DSC. The DSC purity determination software constructs a van't Hoff plot for the calculation of purity. [c] Onset decomposition temperatures (10% mass loss) were determined with a TGA in an N_2 atmosphere. [d] Onset decomposition temperatures (10% mass loss) were determined with a TGA in an air atmosphere. [e] T_g was determined by heating at 10 °C/min from 35 to 250 °C followed by cooling to −50 °C and heating again at 10 °C/min to 250 °C.

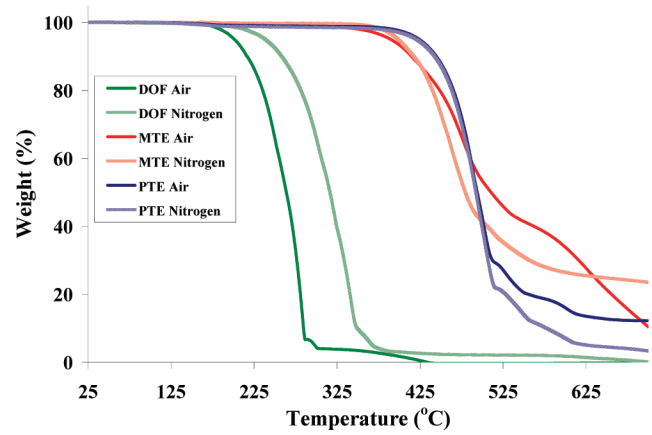

Figure 1. TGA curves of DOF, MTE, and PTE monomers in an air and N_2 atmosphere at a heating rate of 10 °C/min.

washed with copious amounts of distilled water. When completely dry, the powder was washed a further three times with a total of 200 mL of diethyl ether, giving a fine off-white powder (2.68 g, 99%). ^{1}H NMR (500 MHz, d_6-DMSO): δ 8.01 (d, J = 8.0 Hz, 2 H); 7.95 (s, 2 H); 7.72−7.50 (m, 8 H); 7.40−7.25 (m, 12 H); 6.41 (s, 2 H); 6.34 (t, J = 6.1 Hz, 2 H); 6.20 (d, J = 5.4 Hz, 2 H); 6.11 (d, J= 5.6 Hz, 2 H); 5.20 (s, 10 H). ^{13}C NMR (125 MHz, d_6-DMSO): δ 153.06, 152.69, 152.22, 141.61, 137.80, 132.22, 131.56, 131.53, 130.77, 129.83, 128.69, 126.43, 123.23, 121.59, 120.68, 120.44, 84.36, 77.69, 74.14, 73.72, 68.01, 64.27. HRMS Calculated for $C_{59}H_{42}O_4Br_2Fe_2$ [M^{2+} = M-2PF_6]: 1084.013 76. Found: 1084.013 00. Elemental Analysis for $C_{59}H_{42}O_4Br_2Fe_2P_2F_{12}$: C, 51.49; H, 3.08. Found: C, 49.75; H, 3.30.

*Synthesis of PTE (**7a**).* 2,7-Dibromo-9,9′-bis[4-(η^6-1,4-diphenoxy-η^5-cyclopentadienyliron hexafluorophosphate)benzene] (PFBC) (1.00 g, 0.73 mmol) was added to each of five 20 mL microwave vials followed by 10 mL of DMF, 10 mL of acetonitrile, 0.92 g of dimethylglyoxime, and a stir bar, yielding a brown solution. The vial was capped and placed in a microwave reactor for 12 min at 200 °C. The resulting opaque black solutions were poured into 600 mL of a 10% HCl(aq) solution and stirred for 5 h before being filtered over a Buchner funnel, yielding a brown filtrate and black residue. The black residue was dried before being suspended in 75 mL of toluene and filtered through Celite. The Celite was washed with an additional 75 mL of toluene, giving a pale yellow filtrate that after evaporation yielded a yellow solid. The solid was dissolved in a minimal amount of dichloromethane and added

Scheme 3. Synthesis of PPTE and PMTE via Nickel-Catalyzed Yamamoto Coupling Protocol (8a or 8b)[a]

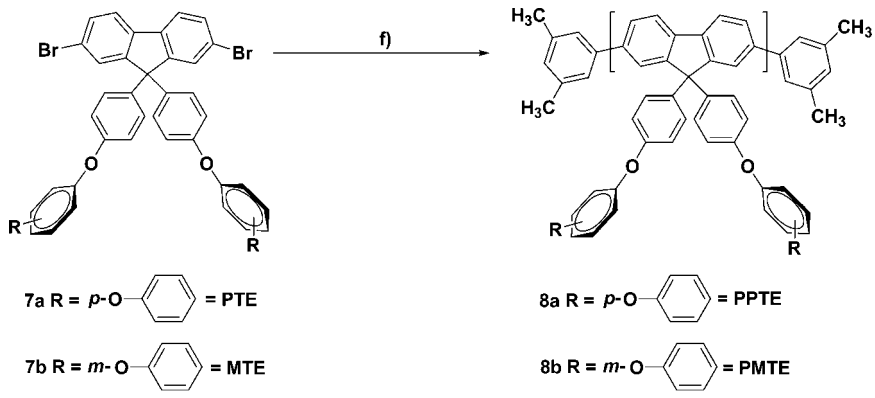

[a] (f) Combine **7a** or **7b**, DMF/toluene ~ 1:2, $Ni(cod)_2$, 2,2′-bipyridyl, 1,5-cyclooctadiene, 5-bromo-*m*-xylene in a microwave vial and heat for 10 min at 230 °C.

Table 2. Weight-Average Molecular Weight (M_w), Polydispersity Index (PDI), Glass Transition Temperature (T_g), Decomposition Temperature T_d, UV−vis Absorption Maxima ($\lambda_{abs,max}$), and Photoluminescence Maxima ($\lambda_{PL,max}$) of Polymers

polymer	M_w[a]	PDI[a]	T_g (°C)[b]	T_d (°C)[c]	$\lambda_{abs,max}$ (nm)[d] solution	$\lambda_{abs,max}$ (nm)[e] film	$\lambda_{PL,max}$ (nm)[d] solution	$\lambda_{PL,max}$ (nm)[e] film
PMTE	12 000	1.8	98	515 (515)[g]	376	390	420	430
PPTE	36 000	3.9	184	534 (528)[g]	374	387	420	440
PFO[f]	52 000	2.2	~50	420	387	390	416	434

[a] M_w and PDI values were determined using GPC in THF with polystyrene standards. [b] T_g (°C) values were determined with DSC at a heating rate of 10 °C/min after heating in vacuum at 100 °C for 24 h. [c] Onset decomposition temperatures (10% mass loss) were determined with TGA in N_2. [d] Solution spectra were measured in toluene with a concentration of 0.001% w/v for $\lambda_{abs,max}$ and 0.00001% w/v for $\lambda_{PL,max}$. [e] Films were drop-coated from toluene solution (1% w/v), and the first vibronic transition is displayed. [f] PFO was purchased from American Dye Source. [g] These values correspond to the second weight loss seen in Figure 3 from the first TGA run.

dropwise to 500 mL of 90% ethanol, resulting in a white precipitate. The combined white solids were filtered over a Buchner funnel and washed twice with a total of 1000 mL of 100% ethanol (1.06 g, 34%). ^{1}H NMR (500 MHz, $CDCl_3$): δ 7.59 (d, J = 9.0 Hz, 2 H); 7.49 (m, J = 1.5 Hz, 4 H); 7.33 (m, J = 7.5, 1.0 Hz, 4 H); 7.10 (m, J = 9.0, 2.0 Hz, 6 H); 6.99 (m, J = 2.0 Hz, 12 H); 6.87 (m, J = 9.0, 2.5 Hz, 4 H). ^{13}C NMR (125 MHz, $CDCl_3$): δ 157.71, 157.29, 153.26, 153.08, 152.06, 138.60, 137.96, 131.06, 129.78, 129.31, 123.12, 121.95, 121.70, 121.02, 120.49, 118.39, 117.78, 64.54. HRMS Calculated for $C_{49}H_{32}Br_2O_4$: 842.066 18. Found: 842.066 19. Elemental Analysis for $C_{49}H_{32}Br_2O_4$: C, 69.68; H, 3.82. Found: C, 69.15; H, 3.82.

*Synthesis of MTE (**7b**).* 2,7-Dibromo-9,9-bis[4-(η^6-1,3-diphenoxy-η^5-cyclopentadienyliron hexafluorophosphate)benzene] (MFBC) (1.00 g, 0.73 mmol) was added to a 30 mL microwave vial followed by 10 mL of DMF, 10 mL of acetonitrile, 0.92 g of dimethylglyoxime, and a stir bar, yielding an orange/red solution. The vial was capped and placed in a microwave reactor for 12 min at 200 °C. The resulting opaque black solution was poured into 120 mL of a 10% HCl(aq) solution and stirred for 5 h before being filtered over a Buchner funnel, yielding a red/brown filtrate and black residue. The black residue was dried before being suspended in 15 mL of toluene and filtered through Celite. The Celite was washed with an additional 15 mL of toluene, giving a light orange filtrate that after evaporation yielded a light orange solid. The solid was dissolved in a minimal amount of dichloromethane and added dropwise to 100 mL of 90% ethanol, resulting in a white precipitate. 10 mL of distilled water was then added to the 100 mL of 90% ethanol to help coagulate any remaining material. The combined white solids were filtered over a Buchner funnel and washed twice with a total of 200 mL of 100% ethanol (0.40 g, 60%). ^{1}H NMR (400 MHz, $CDCl_3$): δ 7.59 (dd, J = 7.6, 0.8.Hz, 2H); 7.49 (dd, J = 7.6, 2 Hz, 2 H); 7.48 (s, 2 H); 7.33 (t, J = 7.6 Hz, 4 H); 7.25 (t, J = 8.0 Hz, 2 H); 7.10 (d, J = 8.8 Hz, 4 H); 7.10 (t, J = 7.6 Hz, 2 H); 7.02 (d, J = 7.6 Hz, 4H); 6.90 (d, J = 8.4 Hz, 4 H); 6.73 (m, J = 7.8 Hz, 4 H); 6.68 (t, J = 2.4 Hz, 2 H). ^{13}C NMR (100 MHz, $CDCl_3$): δ 158.63, 157.97, 156.50, 156.05, 152.99, 139.13, 137.86, 131.01, 130.36, 129.74, 129.27, 129.21, 123.62, 121.89, 121.63, 119.20, 118.65, 118.57, 113.55, 113.44, 109.58, 64.58. HRMS Calculated for $C_{49}H_{32}Br_2O_4$: 842.066 18. Found: 842.066 19. Elemental Analysis for $C_{49}H_{32}Br_2O_4$: C, 69.68; H, 3.82. Found: C, 69.41; H, 3.86.

*Synthesis of PPTE (**8a**).* PTE (0.200 g, 0.237 mmol) was placed in a Biotage 10−20 mL microwave vial along with byp (0.098 g, 0.632 mmol), $Ni(cod)_2$ (0.168 g, 0.611 mmol), and 1,5-cyclooctadiene (0.08 mL, 0.7 mmol) inside an argon-filled glovebox forming a purple paste. The mixture was diluted with 9 mL of DMF and 14 mL of toluene, followed by 5-bromo-*m*-xylene (1.6 μL, 0.0118 mmol) as an end-capping agent, resulting in a red solution. The vial was capped and irradiated in a Biotage Initiator microwave system for 10 min at an internal temperature of 230 °C. The purple/black contents of the vial were poured into 150 mL of methanol, and the polymer was allowed to agglomerate overnight. The blue/gray slurry was transferred to the thimble of a Soxhlet extractor and washed with 300 mL of acetone for 24 h followed by an extraction with 300 mL of toluene for 24 h. The toluene was removed with a rotary evaporator, yielding a green flakey solid (0.160 g, 98%). The solid was subsequently dried in a vacuum oven at ~100 °C for 24 h. ^{1}H NMR and ^{13}C NMR spectra were acquired after filtering a toluene-d_8 solution through a 0.2 um Millipore Millex-GN filter. ^{1}H NMR (500 MHz, toluene-d_8): δ 7.9−7.8 (m, 2H) 7.7−7.5 (m, 6 H); 7.4−7.1 (m, 7 H); 6.9−6.4 (m, 33 H). ^{13}C NMR (125 MHz, toluene-d_8): δ 158.27, 157.65, 157.50, 153.46, 153.39, 153.27, 152.94, 152.66, 152.49, 141.61, 140.61, 140.46, 140.05, 139.51, 129.96, 129.82, 129.28, 129.16, 128.47, 128.23, 125.61, 123.17, 121.34, 121.20, 120.74, 118.68, 117.98, 65.22. MALDI-TOF mass spectrometry polymer repeat unit ($C_{49}H_{32}O_4$): Calculated: 684.776. Found: ~685 amu. Elemental Analysis calculated for $C_{49}H_{32}O_4$ polymer repeat unit: C, 85.94; H, 4.71. Found: C, 80.64; H, 5.37. Also found 0.42% nitrogen.

*Synthesis of PMTE (**8b**).* MTE (0.150 g, 0.178 mmol) was placed in a Biotage 10−20 mL microwave vial along with bpy (0.074 g, 0.474 mmol), $Ni(COD)_2$ (0.126 g, 0.458 mmol), and 1,5-cyclooctadiene (0.06 mL, 0.5 mmol) inside an argon-filled glovebox forming a purple paste. The mixture was diluted in 6.8 mL of DMF and 10.5 mL of toluene, followed by 5-bromo-*m*-xylene (1.2 μL, 0.00885 mmol) as an end-capping agent, forming a brown solution. The vial was capped and irradiated in a Biotage Initiator microwave

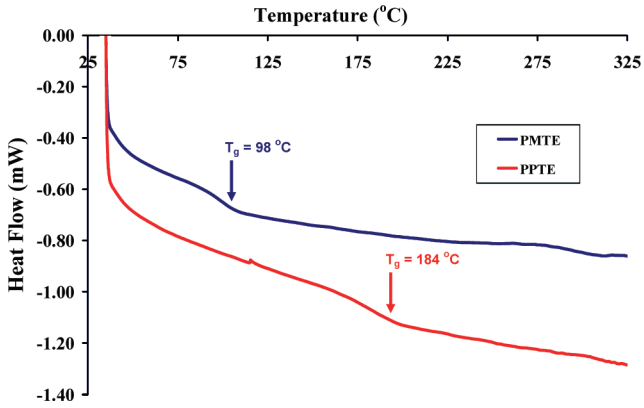

Figure 2. DSC traces of PPTE (red) and PMTE (blue) at a heating rate of 10 °C/min. The samples were dried for 24 h at ca. 100 °C in a vacuum oven prior to analysis.

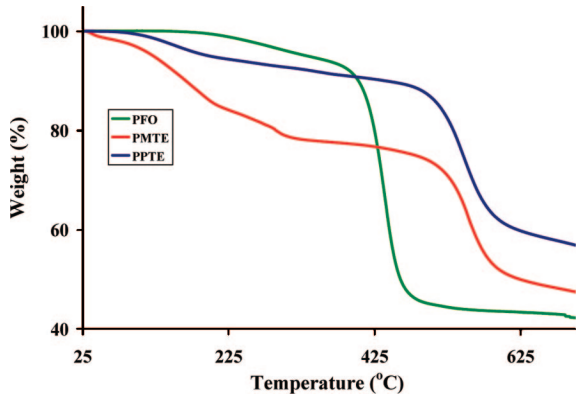

Figure 3. TGA traces of PFO (green), PMTE (red), and PPTE (blue) in a N_2 atmosphere at a heating rate of 10 °C/min after being dried for 24 h in vacuum at ca. 100 °C. The traces correspond to a single TGA heating run.

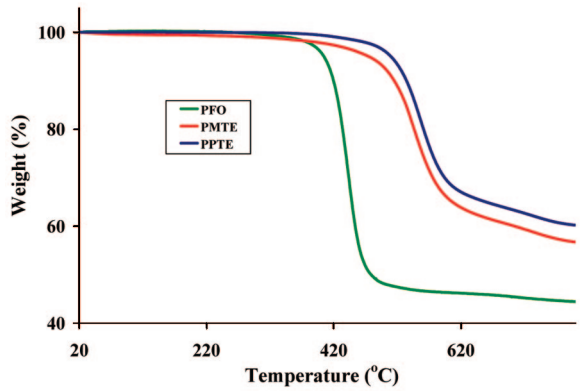

Figure 4. TGA traces of PFO (green), PMTE (red), and PPTE (blue) in a N_2 atmosphere at a heating rate of 10 °C/min. The traces correspond to material that has been pretreated by heating the sample in a TGA crucible from 25 to 320 °C, cooling it back down to 25 °C, and heating the sample again to 700 °C.

system for 10 min at an internal temperature of 230 °C. The purple/green contents of the vial were poured over a 1:1:1 solution of acetone:methanol:HCl(conc), forming a cloudy white solution and brown oil. The polymer was extracted with 4 × 100 mL portions of toluene, resulting in an orange organic layer that was subsequently dried over magnesium sulfate. Following gravity filtration the toluene was removed by rotary evaporator, yielding a brown flakey solid (0.111 g, 89%). The solid was subsequently dried in a vacuum oven at ~100 °C for 24 h. ^{1}H NMR and ^{13}C NMR spectra were acquired after filtering a $CDCl_3$ solution through a 0.2 μm

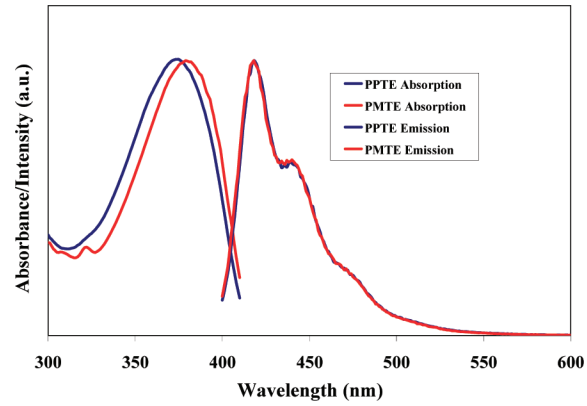

Figure 5. UV−vis and PL spectra (λ_{ex} = 350 nm) of a 0.001% w/v and a 0.00001% w/v toluene solution of PPTE (blue) and PMTE (red).

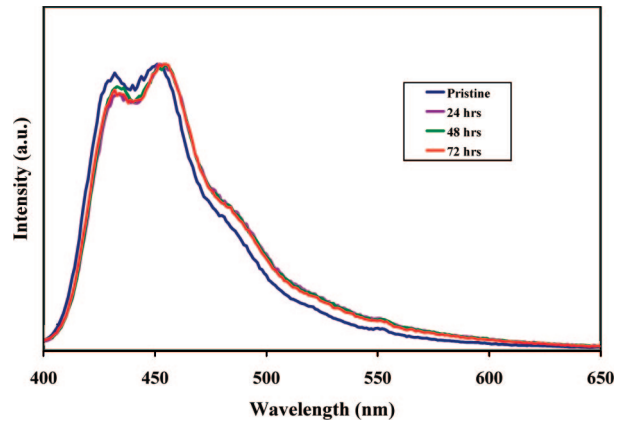

Figure 6. PL spectra (λ_{ex} = 350 nm) of a drop-coated PPTE film annealed at 200 °C for indicated times in an N_2-filled glovebox.

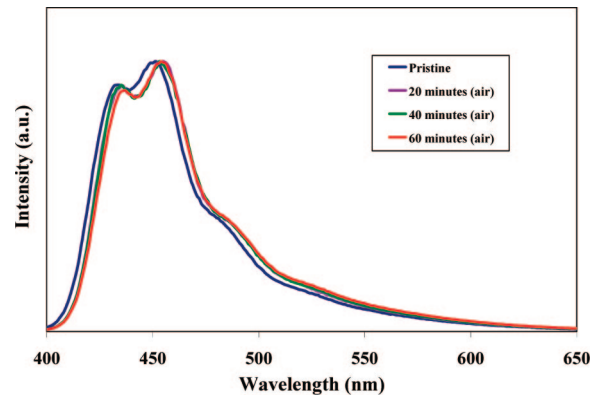

Figure 7. PL spectra (λ_{ex} = 350 nm) of a drop-coated PPTE film annealed at 150 °C for indicated times under ambient conditions.

Millipore Millex-GN filter. ^{1}H NMR (400 MHz, $CDCl_3$): δ 7.92−7.70 (m, 2H) 7.68−7.45 (m, 4 H); 7.44−7.26 (m, 4 H); 7.24−7.03 (m, 8 H); 7.02−6.94 (m, 4 H); 6.92−6.80 (m, 4 H); 6.76−6.56 (m, 6 H). ^{13}C NMR (100 MHz, $CDCl_3$): δ 158.68, 158.43, 158.17, 156.55, 155.86, 155.70, 141.00, 130.30, 129.75, 129.73, 129.45, 129.36, 129.24, 126.94, 126.05, 124.60, 123.57, 119.20, 119.18, 118.58, 113.45, 113.32, 113.26, 113.22, 109.55, 109.45, 64.6. MALDI-TOF mass spectrometry polymer repeat unit ($C_{49}H_{32}O_4$): Calculated: 684.776. Found: ~685 amu. Elemental Analysis calculated for $C_{49}H_{32}O_4$ polymer repeat unit: C, 85.94; H, 4.71. Found: C, 75.09; H, 5.80. Also found 2.03% nitrogen.

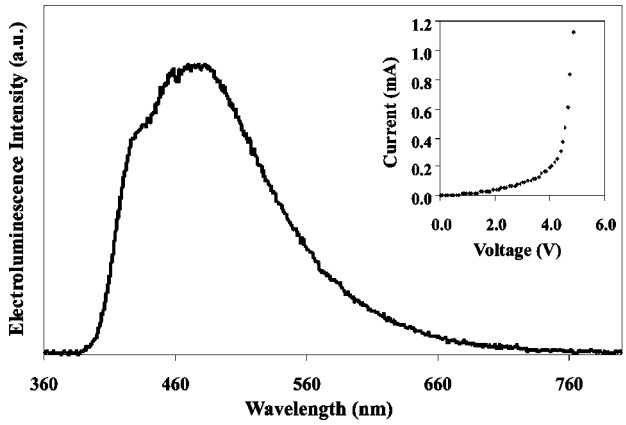

Figure 8. Electroluminescence spectrum and current−voltage ($I-V$) (inset) characteristics of a PLED fabricated with PMTE as the emitting layer.

Results and Discussion

Synthesis of PTE and MTE Monomers. Intermediate compound 2,7-dibromofluoren-9-one[39] (**2**) and target precursor compound 2,7-dibromo-9,9′-di(4-hydroxyphenyl)-9*H*-fluorene[40] (**3**), as shown in Scheme 1, were prepared according to literature procedures and characterized with ^{1}H and ^{13}C NMR spectroscopy and electron-impact (EI) mass spectrometry. The crystal structure of **3** was reported previously.[41]

3 was subsequently reacted with **4a** or **4b**,[42] as outlined in Scheme 2, to generate *p*-intermediate-bimetallic-complex (PIBC) **5a** or *m*-intermediate-bimetallic-complex (MIBC) **5b.** Isolation of PIBC or MIBC was not necessary; both were further reacted with additional phenol to produce *p*-final-bimetallic-complex (PFBC) **6a** or *m*-final-bimetallic-complex (MFBC) **6b**, respectively. The $CpFe^+$ moieties on the bimetallic complexes PFBC and MFBC were removed via microwave irradiation to generate *p*-tetra-ether (PTE) **7a** and *m*-tetra-ether (MTE) **7b**, respectively. Compounds **5**−**7a**,**b** were characterized with ^{1}H and ^{13}C NMR spectroscopy, high-resolution mass spectrometry (HRMS), and elemental analysis (EA) (Figures SI-1 to SI-10 of the Supporting Information).

Thermal and Oxidative Stability of PTE and MTE Monomers. TGA of PTE, MTE, and purified 2,7-dibromodioctylfluorene (DOF), in N_2 and air, provided insight into the thermal and oxidative stability of AE-functionalized monomers as well as direct comparison with DOF. Table 1 summarizes and Figure 1 shows the onset of decomposition (10% weight loss) of MTE and PTE in N_2 and air occurs at substantially higher temperatures (ca. 150 °C) than for DOF. We attribute this increased stability to the stabilizing influence of the AE moieties. We also note the onset of decomposition of PTE and MTE is approximately the same in both N_2 and air, in stark contrast to DOF. This may indicate the lack of a readily accessible decomposition pathway for AE-containing PTE and MTE.

Thermal Phase Behavior of PTE and MTE Monomers. Differential scanning calorimetry (DSC) provides insight into the phase behavior of PTE and MTE monomers. Table 1 summarizes the melting temperatures (T_m), purity, and glass transition temperatures (T_g) of PTE and MTE as determined by DSC. PTE and MTE exhibit well-defined melting temperatures (T_m) of 166 and 181 °C, respectively, when heated from 35 to 250 °C on the first heating cycle (Figures SI-11 and SI-12 of the Supporting Information). Upon cooling (10 °C/min) and reheating (10 °C/min) the sample, the well-defined melting temperatures are replaced by PTE and MTE glass transition temperatures of 78 and 53 °C, respectively. The appearance of PTE and MTE glass transitions indicates that the cooling rate employed (10 °C/min) during the DSC run was faster than nucleation and subsequent crystal growth. Similar behavior has been noted for glass-forming, high-T_g, bulky spiro compounds in which the crystallization kinetics are slowed.[43] Importantly, the higher T_g's exhibited by PTE and MTE are expected to translate into AE-based polymers with higher T_g's than PFO[44] and increased emission stability.

Synthesis of PPTE and PMTE Polymers. The role of microwave technology in organic synthesis is expanding greatly and is now beginning to be utilized in organic polymer syntheses. One of the primary advantages of this synthetic technique is significantly decreased reaction times that make high throughput material synthesis viable. Highlighting this point, the first report of a PF-type polymer synthesis using microwave irradiation appeared in 2002.[45] Carter outlined the successful polymerization of alkyl-substituted PF materials in 10 min—a dramatic advancement over the traditional 3−4 days required for conventional thermal heating. We employed a microwave-based approach for the polymerization of our AE-functionalized PTE and MTE monomers and successfully prepared poly-*p*-tetra-ether (PPTE) **8a** and poly-*m*-tetra-ether (PMTE) **8b**, as shown in Scheme 3. PPTE and PMTE were characterized with ^{1}H and ^{13}C NMR spectroscopy (Figures SI-13 to SI-16), gel permeation chromatography (GPC) (Figures SI-17 and SI-18), MALDI-TOF mass spectrometry (Figures SI-19 and SI-20), and elemental analysis (EA).

Thermal Phase Behavior of PPTE and PMTE Polymers. The glass transition temperature (T_g) of PPTE and PMTE was evaluated with DSC at a heating rate of 10 °C/min, as summarized in Table 2 and shown in Figure 2. The glass transition temperature of PPTE (184 °C) is substantially higher than PMTE (98 °C), which we attribute to PPTEs higher molecular weight and more symmetric side chains.

Thermal Stability Characterization of PPTE and PMTE Polymers. TGA investigations of PPTE, PMTE, and commercially available PFO, in an N_2 atmosphere, were conducted to gain direct comparison of their thermal stability. Figure 3 and Table 2 show PPTE and PMTE lose approximately 10% and 20% of their weight prior to plateauing at ca. 320 °C. These polymers subsequently undergo another weight loss, which we attribute to decomposition of the polymer, at 528 and 515 °C, respectively.

If PPTE and PMTE are first heated to 320 °C, cooled to 25 °C, and reheated to 700 °C, similar decomposition temperatures (534 and 515 °C) are observed (see Figure 4).

While the weight loss up to 320 °C could be attributed to the liberation of volatile impurities (e.g., solvent) remaining following synthesis and work-up, placing PPTE and PMTE in a vacuum oven at ca. 100 °C for 24 h did not address this issue. Elemental analysis of PPTE and PMTE revealed carbon content to be ca. 5% and 10% below theoretically predicted values, and nitrogen contamination of ca. 0.5 and 2.0%, respectively, was noted. Ongoing investigations in our laboratory are focused on gaining a better understanding of the structure of these polymers (i.e., end-group analysis) using high-resolution MALDI-FTICR.

PPTE and PMTE, shown in Figure 4, exhibit significantly higher thermal decomposition temperatures than PFO, indicating AE moieties substantially improve the thermal and oxidative stability of PFs. The improvement in thermal stability of our AE-containing polymers (PPTE and PMTE) over PFO is smaller (ca. 100 °C) than the difference in stability between the AE-containing monomers and DOF (ca. 150 °C), indicating that monomer stability does not necessarily quantitatively correlate with polymer stability.

Photoluminescence Stability of PPTE and PMTE Polymers. Figure 5 and Table 2 show solution UV−vis and photoluminescence (PL) spectra of PPTE and PMTE. These spectra are consistent with polymer formation and similar to those obtained for alkyl-substituted PF materials (e.g., PFO).

Films of PPTE, PMTE, and PFO drop-coated and/or spin-coated from 1% w/v toluene solutions onto quartz substrates were evaluated for thermal and morphological stability upon thermal annealing in an N_2 atmosphere. In an effort to ensure removal of excess toluene, films were dried in ambient prior to drying in vacuo (ca. 30 mTorr) for 24 h. Upon annealing a PFO film at 200 °C, in an inert N_2 atmosphere, the PL spectrum continuously evolved over 80 h, resulting in three changes to the spectrum: (1) the contributions to the spectrum from each of the vibronic components change, (2) a shift in the relative positions of these transitions, and (3) the intensity of the PL, in the green spectral region (ca. 550 nm), increases.[46] These changes are well established and have been attributed to polymer chain reordering and excimer formation.[47] In contrast to commercial PFO, PPTE and PMTE display spectral stability when annealed under identical conditions, as shown in Figure 6 and Figure SI-21 (Supporting Information).

Thermal annealing of PPTE, PMTE, and PFO in air show very different effects on the PL spectra. PFO shows a dramatic increase in green emission (ca. 550 nm) after annealing in air for 60 min at 150 °C, and the resulting green emission visibly dominates film color after only 20 min of thermal stressing.[46] In contrast, the PL spectra of PPTE and PMTE exhibit negligible change under identical conditions which severely degrade PFO response, as shown in Figure 7 and Figure SI-22 (Supporting Information). We attribute the increased stability to the stabilizing influence of the AE moieties at the 9-position in PPTE and PMTE.

Electroluminescence and Current−Voltage (*I*−*V*) Characteristics of PMTE Polymer. Proof-of-concept polymer light-emitting diodes (PLEDs) with PMTE as the emitting layer were fabricated with the following sandwich structure: ITO/PEDOT-PSS/PMTE/Ca/Al. The electroluminescence spectrum reproduces the photoluminescence spectrum and under ambient conditions did not shift during device testing (ca. 30 min). PMTE exhibited turn-on voltages of ca. 4.5 V and exhibited blue electroluminescence as shown in Figure 8. Ongoing investigations will focus on further device stressing in a variety of environments and temperature regimes.

Conclusions

The direct incorporation of AE functionality into PF materials at the 9-position has allowed for the preparation of thermally stable materials with excellent oxidative stability. We are currently exploring $CpFe^+$ chemistry in efforts to prepare additional AE-containing PF materials possessing subtle structural features in an effort to investigate more fully the solution and solid state properties of these polymers. Initial electroluminescence results support further exploration of this material system for PLED applications.

Acknowledgment. The authors acknowledge funding from the Natural Sciences and Engineering Research Council of Canada (NSERC), Canada Foundation for Innovation (CFI), the Informatics Circle of Research Excellence (iCORE), Micralyne, Inc., and the University of Alberta. M.F. acknowledges the Killam Trusts, Alberta Ingenuity, and NSERC for fellowship support. C. W. Moffat and R. Lister are thanked for assistance with EA and TGA. E. J. Henderson and Dr. C. M. Hessel are also thanked for useful discussions. J. Kelly is also thanked for assistance with design of the table of contents graphic.

Supporting Information Available: Experimental procedure for all monomers and polymers and ^1H and ^{13}C NMR spectra, MALDI-TOF, and GPC traces. This material is available free of charge via the Internet at http://pubs.acs.org.

References and Notes

(1) Niu, Y. H.; Hou, Q.; Cao, Y. *Appl. Phys. Lett.* **2002**, *81*, 634.
(2) Anni, M. *Appl. Phys. Lett.* **2008**, *93*, 023308.
(3) Yap, B. K.; Xia, R.; Campoy-Quiles, M.; Stavrinou, P. N.; Bradley, D. D. C. *Nat. Mater.* **2008**, *7*, 376–380.
(4) Ryu, G.; Xia, R.; Bradley, D. D. C. *J. Phys.: Condens. Matter* **2007**, *19*, 056205.
(5) Xia, R.; Heliotis, G.; Hou, Y.; Bradley, D. D. C. *Org. Electron.* **2003**, *4*, 165–177.
(6) Heliotis, G.; Xia, R.; Bradley, D. D. C.; Turnbull, G. A.; Samuel, I. D. W.; Andrew, P.; Barnes, W. L. *Appl. Phys. Lett.* **2003**, *83*, 2118–2120.
(7) Zhu, L.; Yang, C.; Zhang, W.; Qin, J. *Polymer* **2008**, *49*, 217–224.
(8) Xing, C.; Shi, Z.; Yu, M.; Wang, S. *Polymer* **2008**, *49*, 2698–2703.
(9) Yu, M.; He, F.; Tang, Y.; Wang, S.; Li, Y.; Zhu, D. *Macromol. Rapid Commun.* **2007**, *28*, 1333–1338.
(10) Grigalevicius, S.; Forster, M.; Ellinger, S.; Landfester, K.; Scherf, U. *Macromol. Rapid Commun.* **2006**, *27*, 200–202.
(11) Mondal, C. K.; Lee, J. Y. *J. Theor. Comput. Chem.* **2006**, *5*, 857–869.
(12) Zhou, X. H.; Yan, J. C.; Pei, J. *Macromolecules* **2004**, *37*, 7078–7080.
(13) Gulbinas, V.; Minevičiūt•e, I.; Hertel, D.; Wellander, R.; Yartsev, A.; Sundström, V. *J. Chem. Phys.* **2007**, *127*, 144907.
(14) Sung, Y. C.; Grimsdale, A. C.; Jones, D. J.; Watkins, S. E.; Holmes, A. B. *J. Am. Chem. Soc.* **2007**, *129*, 11910–11911.
(15) Beljonne, D.; Pourtois, G.; Shuai, Z.; Hennebicq, E.; Scholes, G. D.; Brédas, J. L. *Synth. Met.* **2003**, *137*, 1369–1371.
(16) Suh, H.; Jin, Y.; Park, S. H.; Kim, D.; Kim, J.; Kim, C.; Kim, J. Y.; Lee, K. *Macromolecules* **2005**, *38*, 6285–6289.
(17) Misaki, M.; Chikamatsu, M.; Yoshida, Y.; Azumi, R.; Tanigaki, N.; Yase, K.; Nagamatsu, S.; Ueda, Y. *Appl. Phys. Lett.* **2008**, *93*, 023304.
(18) Becker, K.; Lupton, J. M.; Feldmann, J.; Nehls, B. S.; Galbrecht, F.; Gao, D.; Scherf, U. *Adv. Funct. Mater.* **2006**, *16*, 364–370.
(19) Amara, J. P.; Swager, T. M. *Macromolecules* **2006**, *39*, 5753–5759.
(20) Chan, K. L.; McKiernan, M. J.; Towns, C. R.; Holmes, A. B. *J. Am. Chem. Soc.* **2005**, *127*, 7662–7663.
(21) Cho, H. J.; Jung, B. J.; Cho, N. S.; Lee, J.; Shim, H. K. *Macromolecules* **2003**, *36*, 6704–6710.
(22) Chou, C. H.; Hsu, S. L.; Dinakaran, K.; Chiu, M. Y.; Wei, K. H. *Macromolecules* **2005**, *38*, 745–751.
(23) Setayesh, S.; Grimsdale, A. C.; Weil, T.; Enkelmann, V.; Müllen, K.; Meghdadi, F.; List, E. J. W.; Leising, G. *J. Am. Chem. Soc.* **2001**, *123*, 946–953.
(24) Marsitzky, D.; Vestberg, R.; Blainey, P.; Tang, B. T.; Hawker, C. J.; Carter, K. R. *J. Am. Chem. Soc.* **2001**, *123*, 6965–6972.
(25) Xia, C.; Advincula, R. C. *Macromolecules* **2001**, *34*, 5854–5859.
(26) Cotter, R. J. *Engineering Plastics: A Handbook of Polyarylethers*; Gordan and Breach Science Publishers S.A.: Basel, 1995; p 357.
(27) Mahoney, C. L.; Barnum, E. R.; Kerlin, W. W.; Sax, K. J.; Saari, W. S. *J. Chem. Eng. Data* **1960**, *5*, 172–180.
(28) Jiang, G.; Wu, J.; Yao, B.; Geng, Y.; Cheng, Y.; Xie, Z.; Wang, L.; Jing, X.; Wang, F. *Macromolecules* **2006**, *39*, 7950–7958.
(29) Jiang, G.; Yao, B.; Geng, Y.; Cheng, Y.; Xie, Z.; Wang, L.; Jin, X.; Wang, F. *Macromolecules* **2006**, *39*, 1403–1409.
(30) Ullmann, P. S. *Ber* **1904**, *37*, 853.
(31) Moroz, A. A.; Shvartsberg, M. S. *Russ. Chem. Rev.* **1974**, *43*, 679–689.
(32) Lu, J.; Miyatake, K.; Hlil, A. R.; Hay, A. S. *Macromolecules* **2001**, *34*, 5860–5867.
(33) Sirotkina, E. I.; Nesmeyanov, A. N.; Vol'kenau, N. A. *B. Acad. Sci. USSR CH+* **1970**, *18*, 1413–1417.
(34) Abd-El-Aziz, A. S.; Pereira, N. M.; Winram, D. J.; Sidhu, P.; Kroeker, S. *J. Inorg. Organomet. Polym. Mater.* **2007**, *17*, 275–282.
(35) Abd-El-Aziz, A. S.; Todd, E. K.; Afifi, T. H. *Macromol. Rapid Commun.* **2002**, *23*, 113–117.
(36) Abd-El-Aziz, A. S.; Todd, E. K.; Ma, G. Z. *J. Polym. Sci., Polym. Chem.* **2001**, *39*, 1216–1231.
(37) Abd-El-Aziz, A. S.; De Denus, C. R.; Zaworotko, M. J.; MacGillivray, L. R. *J. Chem. Soc., Dalton Trans.* **1995**, 3375–3393.
(38) Yamamoto, T.; Morita, A.; Miyazaki, Y.; Maruyama, T.; Wakayama, H.; Zhou, Z. H.; Nakamura, Y.; Kanbara, T.; Sasaki, S.; Kubota, K. *Macromolecules* **1992**, *25*, 1214–1223.
(39) Ranger, M.; Leclerc, M. *Macromolecules* **1999**, *32*, 3306–3313.

(40) Lindgren, L. J.; Wang, X.; Inganäs, O.; Andersson, M. R. *Synth. Met.* **2005**, *154*, 97–100.
(41) Nadeau, N.; McFarlane, S.; McDonald, R.; Veinot, J. G. C. *Acta Crystallogr.* **2007**, *E63*, o748–o749.
(42) Khand, I. U.; Pauson, P. L.; Watts, W. E. *J. Chem. Soc. C* **1968**, 2261–2265.
(43) Saragi, T. P. I.; Spehr, T.; Siebert, A.; Fuhrmann-Lieker, T.; Salbeck, J. *Chem. Rev.* **2007**, *107*, 1011–1065.
(44) Grell, M.; Bradley, D. D. C.; Inbasekaran, M.; Woo, E. P. *Adv. Mater.* **1997**, *9*, 798–802.
(45) Carter, K. R. *Macromolecules* **2002**, *35*, 6757–6759.
(46) McFarlane, S. L.; Coumont, L. S.; Piercey, D. G.; McDonald, R.; Veinot, J. G. C. *Macromolecules* **2008**, *41*, 7780–7782.
(47) Schwartz, B. J. *Annu. Rev. Phys. Chem.* **2003**, *54*, 141–172.

MA8022348